NMR imaging of experimental brain abscess: comparison with CT.

M Brant-Zawadzki, D R Enzmann, R C Placone, Jr, P Sheldon, R H Britt, R C Brasch and L A Crooks

AJNR Am J Neuroradiol 1983, 4 (3) 250-253
http://www.ajnr.org/content/4/3/250

NMR Imaging of Experimental Brain Abscess: Comparison with CT

Michael Brant-Zawadzki,[1] Dieter R. Enzmann,[2] Richard C. Placone, Jr.,[2] Philip Sheldon,[1] Richard H. Britt,[3] Robert C. Brasch,[1] and Lawrence A. Crooks[1]

An experimental canine model of a brain abscess induced with alpha-streptococcus was imaged in the cerebritis and capsule stages by computed tomography (CT) with intravenous contrast enhancement and by nuclear magnetic resonance (NMR). An NMR imager equipped with a superconducting magnet operating at 3.5 kG was used for several imaging techniques. The NMR images were compared with the CT scans and with gross and microscopic neuropathologic findings. CT showed enhancement of the inflammatory focus at the site of capsule formation while the necrotic center retained its low-density appearance. Spin-echo NMR images demonstrated the presence and extent of abnormal infected brain tissue more accurately than contrast-enhanced CT. Spin-echo images showed the necrotic center, the surrounding inflammatory zone, and peripheral edema without discriminating distinctly between the latter two zones. Inversion-recovery NMR images depicted a lesion of lesser extent, showing the necrotic center circumscribed by the surrounding edematous brain tissue. The inversion-recovery technique was best for demonstrating gray- and white-matter contrast in normal brain and depicted edema as loss of contrast between the gray and white matter. NMR offers some advantages over CT in imaging brain abscess, and the variety of NMR imaging techniques is useful for characterizing the different pathologic areas.

The rapid development of clinical nuclear magnetic resonance (NMR) imagers has been documented by recent reports from several institutions [1–6]. However, defining the future role of NMR in medical imaging requires studies that compare NMR in specific disease processes with existing modalities such as computed tomography (CT) and especially with actual pathology. NMR images depend on the density of hydrogen nuclei (protons) and the biochemical milieu of those nuclei within tissue rather than on attenuation of ionizing radiation. Because of this fundamental difference, any attempt at drawing conclusions about NMR images by mere comparison with CT is problematical. A basic understanding of the meaning of an NMR image in a particular disease entity is necessary. Correlation with pathologic specimens is a more precise method of assessing the capabilities of a new imaging modality, and reproducible animal models serve this purpose well [7].

We used an established canine model to investigate NMR imaging of brain abscess. The diagnosis and therapy of brain abscess has been altered since the introduction of CT, which has permitted accurate localization and staging of this type of lesion [8]. But repeated CT studies of cerebritis or abscess are often necessary to monitor the effects of specific forms of therapy. If NMR can offer the same sensitivity for detection and staging as CT, its lack of ionizing radiation and elimination of the need for intravenous contrast agents would make NMR the preferred modality for diagnosis and evaluation of brain abscess.

Materials and Methods

Mongrel dogs weighing about 25–40 kg were studied after induction of brain abscess with alpha-streptococcus by a previously described technique [9, 10]. Two dogs were imaged in the cerebritis stage of the infection (3–8 days after inoculation) and two in the capsule stage (14 and 22 days postinoculation, respectively). The animals were sacrificed at each stage after imaging and histologic examinations were performed using the previously reported technique [9, 10]. One dog imaged in the capsule stage had suboptimal anatomic correlation for spin-echo NMR images for technical reasons.

Coronal CT scans were obtained with a Varian CT scanner after intravenous bolus injection of Conray 60% (dose, 2 ml/kg). Section thickness was 10 mm. Serial scans were obtained at 0, 10, 20, 30, 45, and 60 min after contrast injection.

NMR imaging was performed on a 3.5 kG superconducting magnet using a coil with an aperture of 25 cm [11]. Spatial resolution was 1.7 mm on a 128 × 128 matrix. Five sequential coronal sections, each 7 mm thick, were sampled in a 13 min period. Four separate images were obtained for each coronal section on the basis of the various instrument parameters used in our spin-echo technique [11]. In addition, inversion-recovery images with a repeated imaging sequence were obtained for the same five sections.

The spin-echo image yielding the highest signal-to-noise ratio data was used for visual correlation with the inversion-recovery images, CT scans, and pathologic findings in the same section. T_1 and T_2 relaxation times for the lesion were sampled and compared with readings for normal brain tissue in the same NMR image in an attempt to characterize the nature of tissue alteration attributable to the infection. (In general, tissues with short T_1 and long T_2 relaxation times, respectively, yield high intensity on spin-echo images. How-

This work was supported in part by Diasonics (NMR), Inc., and U.S. Public Health Service grant CA 32850 from the National Cancer Institute.

[1]Department of Radiology and Radiologic Imaging Laboratory, University of California, San Francisco, CA 94143. Address reprint requests to M. Brant-Zawadzki at the Department of Radiology, San Francisco General Hospital, 1001 Potrero Ave., San Francisco, CA 94110.

[2]Department of Radiology, Stanford University School of Medicine, Stanford, CA 94305.

[3]Department of Surgery, Division of Neurosurgery, Stanford University School of Medicine, Stanford, CA 94305.

AJNR 4:250–253, May/June 1983 0195-6108/83/0403-0250 $00.00

Fig. 1.—Right parietal abscess in experimental canine model. Cerebritis stage. **A**, Gross pathologic specimen, postinoculation day 6. Black stain indicates sparse areas of perivascular reticulin without significant capsule formation. Central liquefactive necrotic area was avascular. **B**, Contrast-enhanced coronal CT scan, postinoculation day 5. Thin, weakly-enhancing rim surrounds large area of low density representing avascular necrotic lesion with pus formation. Cerebral edema was identified superomedial and inferior to primary lesion. **C**, Spin-echo NMR image, postinoculation day 6. Same section as **B**. Ring of high intensity surrounds central necrotic area, diffusing into subjacent temporal lobe. **D**, Spin-echo image obtained with instrument parameters emphasizing T_1 relaxation time. Liquefactive necrotic lesion more clearly visualized than in **C**. **E**, Inversion-recovery NMR image, postinoculation day 6. Focal low-intensity region marks site of central necrosis. Loss of gray- and white-matter contrast in area adjacent to lesion suggests edema.

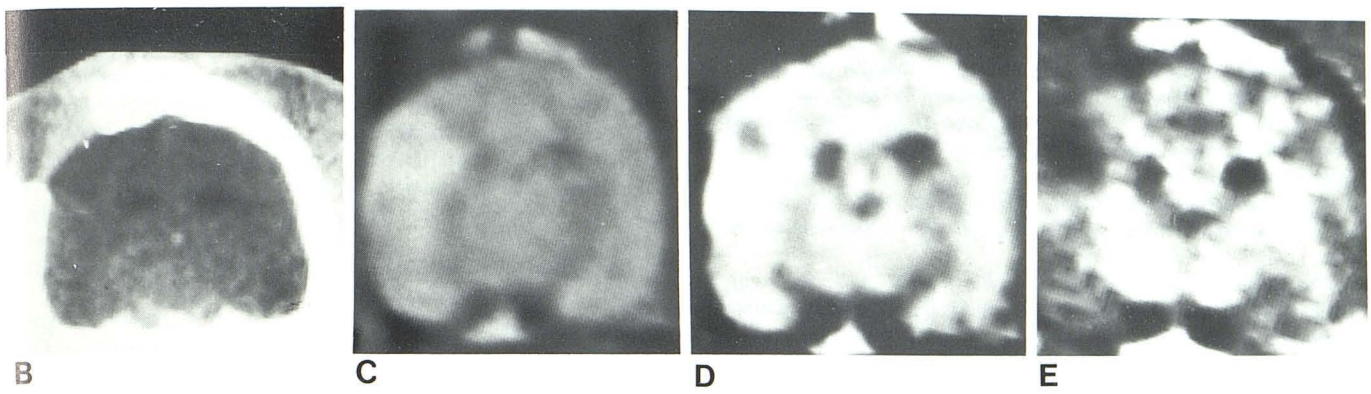

Fig. 2.—Right parietal abscess in experimental canine model. Capsule stage. **A**, Gross pathologic specimen, postinoculation day 14. Black stain marks band of reticulin indicating significant capsule formation. Central necrotic area was avascular and composed of liquefied debris. **B**, Contrast-enhanced coronal CT scan, postinoculation day 13. Typical ring lesion with low-density center. Edema was present, notably superomedial to abscess. **C**, Spin-echo NMR image, postinoculation day 14. Same section as **B**. Central area of low intensity corresponds to liquefactive necrosis on pathologic specimen. Ring of high intensity extending into adjacent brain corresponds to region of capsule formation and peripheral circumscribed edema.

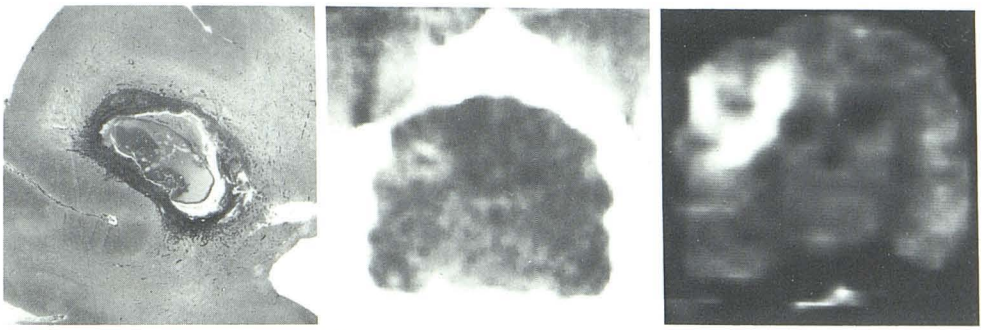

ever, the interplay of the relaxation times and the various imaging sequences is complex, and the interested reader is referred to a recent report from our institution for a thorough discussion of the multiparametric nature of NMR imaging [11].)

Results

Cerebritis Stage

The histologic appearance of this stage was the same as that previously described in this model [9, 10, 12]. A central avascular necrotic area was surrounded by a dense inflammatory zone (fig. 1A) representing the anlage for subsequent capsule formation. This inflammatory zone became rarefied at its periphery with a gradual transition into a region of marked edema that spread out into the adjacent white matter. A small amount of collagen deposition was seen late in this stage.

The CT scans showed ring enhancement corresponding visually to the inflammatory zone described above and surrounding a large area of low attenuation (fig. 1B).

The spin-echo NMR images showed high intensity in both the dense inflammatory zone and the surrounding edematous brain tissue (fig. 1C). The high-intensity region was therefore more extensive than the contrast-enhanced lesion seen on CT. A lower-intensity central area corresponded to the necrotic core. The T_2 relaxation time was markedly prolonged in the peripheral high-intensity zone, and a modest prolongation of T_1 was also noted relative to normal brain. Such a combination is consistent with edematous

brain tissue. The low-intensity necrotic core reflected a markedly prolonged (×3) T_1 relaxation time (fig. 1D). A lengthened T_2 relaxation time was also noted in the core, a factor tending to increase NMR signal intensity on spin-echo images, but the marked T_1 prolongation dominated the signal characteristics [11]. The low-intensity signal in the center of the lesion correlated well with liquefactive necrosis in the later stage of cerebritis, as seen on the pathologic specimens.

The inversion-recovery images depicted the lesion as a central focal area of low intensity (fig. 1E). Loss of the gray- and white-matter contrast in the area adjacent to the lesion was due to edema. Gray-white contrast was optimally demonstrated on inversion-recovery images in the normal portions of the brain.

Capsule Stage

Histologic sections of the capsule stage showed a well circumscribed lesion with a necrotic center surrounded by dense collagenous tissue (fig. 2A). A narrow zone of cerebritis was seen just beyond the capsule. Edema had regressed to an area more immediate to the capsule.

The CT scans showed discrete ring enhancement around an area of low attenuation corresponding to the region of the capsule (fig. 2B).

The spin-echo NMR images (fig. 2C) showed a more circumscribed peripheral high-intensity area than spin-echo images in the cerebritis stage (where the peripheral high-intensity region was diffuse). As in the earlier stage, the necrotic core was represented by a central area of low intensity. The edges of the peripheral high-intensity region were more clearly delineated in this stage.

The inversion-recovery images depicted the lesion as a well circumscribed, very low-intensity area. Gray- and white-matter contrast in the adjacent area was sharper than in the cerebritis stage. T_1 was again greatly lengthened in the area representing the necrotic core of the lesion, while the inflammatory peripheral zone showed lenghened T_2 with only slight T_1 prolongation.

Discussion

Several attributes of an imaging modality used in the evaluation of brain abscess are important. The method must be sensitive. Our preliminary experience with NMR suggests that it would probably be more sensitive than CT in the early detection of cerebritis. This stage is characterized primarily by inflammatory cell infiltration and edema [10], and NMR proved more sensitive than CT in detecting cerebral edema in normal brain tissue adjacent to the necrotic focus of cerebritis. Most patients presenting with brain abscess already have an obvious lesion; therefore, the potential for very early detection is present in only a small number of patients. Specificity (i.e., ability to differentiate the lesion from other pathologies) is also desirable, but is relatively low with CT. Further experience with NMR imaging sequences may lead to improved specificity.

The ability to detect a liquefactive necrotic center in a brain abscess is important from the aspect of treatment, because aspiration of the fluid assists both in identifying the causative organism and in decreasing the associated mass effect of the lesion. The ability to identify an abscess with a well formed capsule aids the surgeon in scheduling excision of the lesion, where indicated. Finally, the ability to follow the response of the lesion to medical therapy in a noninvasive manner is clearly advantageous. At present, the most accurate gauge of a favorable response to therapy is a decrease in the diameter of the capsule's ring enhancement as seen on CT. Although NMR imaging is noninvasive, it offers no clear analog to CT ring enhancement. However, progressive decrease in size of the necrotic center of the lesion as seen on NMR images may serve as a parallel. An NMR sequence that relies heavily on edema for staging the lesion may be less accurate, especially if corticosteroids are used in treatment [13].

The two modalities proved equally able to suggest the development of central necrosis, enabling interventional aspiration. NMR is more specific than CT in this respect since it can distinguish liquefaction from simple edema. NMR depicts cerebral edema as an area of high intensity on spin-echo images, while liquefaction is visualized as a very low-intensity region both on spin-echo and inversion-recovery technique. Both of these pathologic changes appear as low-density areas on CT scans and are thus difficult to differentiate. The pattern of contrast enhancement on multiple sequential scans of the lesion obtained over a 1 hr period allows this differentiation, however.

The spin-echo NMR images were less effective than CT in predicting the eventual site of capsule formation in the cerebritis stage. The dense inflammatory zone was not clearly differentiated from edematous brain tissue on spin-echo images. Accurate measurements on pathologic sections are difficult, since the transition between the inflammatory region and peripheral edema is gradual. Precise quantitative anatomic correlation between pathology and imaging is therefore problematic. However, if it is assumed the capsule would appear in the immediate periphery of the liquefactive center, which was clearly visualized by NMR, the future site of capsule formation was predictable.

Identification of the capsule stage was more problematic in our limited experience with NMR than in time-density analyses of CT scans [9, 10]. Presence of the capsule could only be inferred in the spin-echo images by sharper demarcation of the lesion. The inversion-recovery images showed not only a low-intensity focal area at the site of the lesion but also improved gray-white contrast in the surrounding area.

NMR does have an advantage over CT when repeated examinations are necessary, since the accumulative radiation dose and potential toxicity of contrast agents is not a factor with the former modality. The broad range of imaging techniques and tissue characterization available with NMR may result in improved specificity for brain abscess, once sufficient technical and interpretive experience is gained.

REFERENCES

1. Holland GN, Hawkes RC, Moore WS. Nuclear magnetic resonance (NMR) tomography of the brain: coronal and sagittal sections. *J Comput Assist Tomogr* **1980**;4:429–433
2. Young IR, Burl M, Clarke GJ, et al. Magnetic resonance properties of hydrogen: imaging the posterior fossa. *AJR* **1981**;137:895–901
3. Crooks L, Arakawa M, Hoenninger J, et al. Nuclear magnetic resonance whole-body imager operating at 3.5 KGauss. *Radiology* **1982**;143:169–174
4. Buonanno FS, Pykett IL, Brady TJ, et al. Clinical relevance of two different nuclear magnetic resonance (NMR) approaches to imaging of a low grade astrocytoma. *J Comput Assist Tomogr* **1982**;6:529–535
5. Alfidi RJ, Haaga JR, El Youseff SJ, et al. Preliminary experimental results in humans and animals with a superconducting whole-body nuclear magnetic resonance scanner. *Radiology* **1982**;143:175–181
6. Bydder GM, Steiner RE, Young IR, et al. Clinical NMR imaging of the brain: 140 cases. *AJNR* **1982**;3:459–480, *AJR* **1982**;139:215–236
7. Hansen G, Crooks LE, Davis P, et al. In vivo imaging of the rat

anatomy with nuclear magnetic resonance. *Radiology* **1980**;136:695–700

8. Stevens EA, Norma D, Kramer RA, et al. Computed tomographic brain scanning in intraparenchymal pyogenic abscesses. *AJR* **1978**;130:111–114
9. Enzmann DR, Britt RH, Yeager AS. Experimental brain abscess evolution: computed tomographic and neuropathologic correlation. *Radiology* **1979**;133:113–122
10. Britt RH, Enzmann DR, Yeager AS. Neuropathological and computerized tomographic findings in experimental brain abscess. *J Neurosurg* **1981**;55:590–603
11. Crooks LE, Mills CM, Davis PL, et al. Visualization of cerebral and vascular abnormalities by NMR imaging: the effects of imaging parameters on contrast. *Radiology* **1982**;144:843–852
12. Enzmann DR, Britt RH, Lyons B, et al. High-resolution ultrasound evaluation of experimental brain abscess evolution: comparison with computed tomography and neuropathology. *Radiology* **1982**;142:95–102
13. Brown SB, Brant-Zawadzki M, Eifel P, et al. CT of irradiated solid tumor brain metastases. *Neuroradiology* **1982**;23:127–131